GRID-CONNECTED PHOTOVOLTAIC SYSTEM WITH BATTERY

T. Shimada*, K. Kurokawa*, T. Yoshioka**
*K.Kurokawa Lab., Tokyo University of Agriculture and Technology, 2-24-16 Naka-cho, Koganei, Tokyo, 184-8588, JAPAN
** Japan Storage Battery Co., Ltd. Inobaba-cho, Nishinosho, Kisshoin, Minami-ku, Kyoto, 601-8520, JAPAN

ABSTRACT: In order to solve the problems which are considered to become the hindrance of further spread of photovoltaic systems, and in order to pursue added value, we are studying the grid-connected photovoltaic system which added the storage battery. This time, the simulation program of the grid-connected photovoltaic system for residences with battery was developed since it was necessary in order to propose and optimize new systems. First, a lead-acid battery was modeled by the original method. Next, the program which simulates the electric power flow of each part in the system was developed. Furthermore, as a result of an actual proof examination, since high simulation accuracy was checked, it is reported.

Keywords: 1: Modeling, 2: Simulation, 3: Accuracy.

1. INTRODUCTION

Most of the photovoltaic system for residences, which began to spread at an increasing tempo in recent years, is a grid-connected type. Usually, since this system has no electric storage, the difference between generated and used electric power is processed according to the electric power flow of the distribution system. Therefore, when this system connects to distribution system with high density, the burden of a sudden change of irradiance or a heavy reverse power flow exceeds the throughput of the power distribution system, and the danger that various problems will occur is pointed out. Moreover, since it depends for generated electric power of solar cells on irradiance, if there is no solar radiation at the time of a power failure, residents cannot use electricity. Paying attention to these present conditions, this research is examining the grid-connected photovoltaic system which added the storage battery.

2. MODELING

In this research, the system configuration as shown in Fig.1 is assumed. Here, simulation models are outlined for every element.

2.1 Solar cell model

A standard I-V curve is made by the fundamental equation [1] derived from the equivalent circuit of a solar cell, and the curve is converted into the conditions of arbitrary irradiance and cell temperature [2]. The model is shown in Formulas 1. They are known well and so their explanations are omitted.

2.2 Lead-acid battery model

There is a lead-acid battery model which is widely used in the field of photovoltaics [1]. This model bases on the equivalent circuit shown in Fig.2. As a result of measuring the charge and discharge characteristic, when a charging and discharging current changed a lot, it became clear that accuracy of estimated terminal voltage falls. Then, in this research, it was proposed that the new model (refer to Formulas 2) considers the dependence of internal resistance on the current, and so estimation accuracy was improved. Here, *u*( ) is a unit step function to combine charge and discharge. A detailed modeling method is described in Chapter 3.

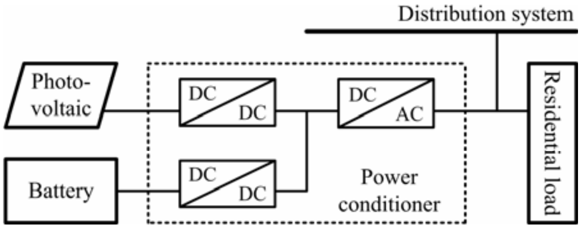

Fig.1: System configuration

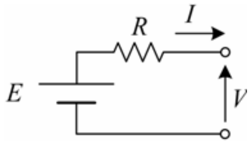

Fig.2: Equivalent circuit of lead-acid battery

$$I = I_{ph} - I_0\left[\exp\left\{q\left(\frac{V + R_s \cdot I}{nkT}\right)\right\} - 1\right] - \frac{V + R_s \cdot I}{R_{sh}}$$
$$I_2 = I_1 + I_{sc}\left(\frac{E_2}{E_1} - 1\right) + \alpha\,(T_2 - T_1)$$
$$V_2 = V_1 + \beta\,(T_2 - T_1) - R_s\,(I_2 - I_1) - K \cdot I_2\,(T_2 - T_1)$$

Formulas 1: Solar cell model

$$V = E - R\,I$$
$$E = E_0 + k_e \ln\left(1 - \frac{Q}{C_T}\right) + E_d \cdot u(-I)$$
$$E_0 = E_{0_0} + E_{0_1}\,T$$
$$k_e = k_{e_0} + k_{e_1}\,T$$
$$E_d = E_{d_0} - E_{d_1} \exp\left\{-E_{d_2}\left(1 - \frac{Q}{C_T}\right)\right\}$$
$$C_T = C_{T_0} - C_{T_1}\,e^{-C_{T_2}\,T}$$
$$R = R_T\left(R_0 + R_1\,e^{-\frac{|I|}{R_2}} + R_g\,G\right)$$
$$R_T = R_{T_0} + R_{T_1}\,e^{-\frac{T}{R_{T_2}}}$$
$$R_0 = (R_{0_0} - R_{0_1}\,Q) \cdot u(I) + \left(Rc_{0_0} + Rc_{0_1}\,e^{-Rc_{0_2}\,Q}\right) \cdot u(-I)$$
$$R_1 = (R_{1_0} - R_{1_1}\,Q) \cdot u(I) + (Rc_{1_0} - Rc_{1_1}\,Q) \cdot u(-I)$$
$$R_2 = (R_{2_0} + R_{2_1}\,Q) \cdot u(I) + (Rc_{2_0} + Rc_{2_1}\,Q) \cdot u(-I)$$
$$Q(t) = Q(t_0) + (1 - G)\int_{t_0}^{t} I(t)\,dt$$
$$G = G_0\,e^{-G_1\,Q} \cdot u(-I)$$

Formulas 2: New model of lead-acid battery

2.3 Power conditioner model

Electric power is lost with three converters shown in Fig.1. These losses were expressed with the quadratic function of each output power according to direction. These 15 coefficients in 5 formulas were determined by the least-squares method from measured data.

3. DETAILED METHOD OF BATTERY MODELING

Procedure for modeling of a lead-acid battery is described in this chapter. And results of the battery simulations are also shown. As the battery, special long life for cycle, 70 Ah VRLA battery [SLC70] made by Japan Storage Battery Co., Ltd. was selected.

3.1 Electromotive force during discharge

Measured discharge characteristic of the battery is shown in Fig.3.1. Expressing this characteristic in the equivalent circuit shown in Fig.2 is considered. In Fig.3.1, although discharging current is changed by half, the amount of change of terminal voltage is not changed by half. This means that internal resistance is not constant and depends on discharging current at that time.

Fig.3.1 is data measured for every second. The integral discharging current Q in each time t is calculated by the following formula.

$$Q(t) = Q(t_0) + \int_{t_0}^{t} I(t)\, dt \qquad 3.1$$

The relations between terminal voltage and discharging current are read from Fig.3.1, and they are plotted on Fig.3.2. The following formula is fitted to 7 groups of the plots as making A, B, C and D into arbitrary constants by the least-squares method.

$$V = A - \left(B + C\, e^{-D\, I}\right) I \qquad 3.2$$

Fitting results are shown with curves in the same figure. Converged A are made into the electromotive force at that discharge state, and are plotted on Fig.3.3. The dependence of electromotive force on the discharge state is expressed with the following formula which considered the Nernst equation.

$$E = E_0 + k_e \ln\left(1 - \frac{Q}{C_T}\right) \qquad 3.3$$

C_T is the capacity when discharging with very small current, and is usually about 1.5 times of rated capacity. The result which determined E_0 and k_e by the least-squares method is shown with a curve in the same figure. Then electromotive force during discharge examination is estimated as shown in Fig.3.4.

3.2 Internal resistance during discharge

Internal resistance R is calculated from Fig.3.4 and current at that time by the following formula.

$$R = \frac{E - V}{I} \qquad 3.4$$

They are plotted on Fig.3.5. It shows that internal resistance decreases with the increase in current but is saturated. Then, the following formula is fitted to 7 groups of these plots by the least-squares method, and the dependence of arbitrary constants in the formula on the discharge state is examined.

$$(R) = R_0 + R_1\, e^{-\frac{I}{R_2}} \qquad 3.5$$

Consequently, it is thought appropriate that internal resistance is expressed with the following formulas.

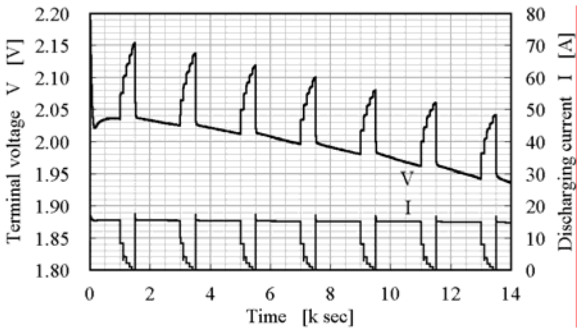

Fig.3.1: Measured discharge characteristic of the battery

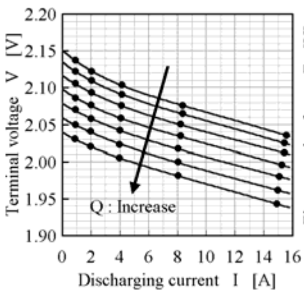

Fig.3.2: Calculating E

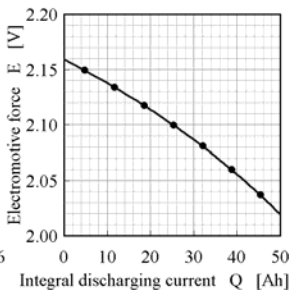

Fig.3.3: Estimated E

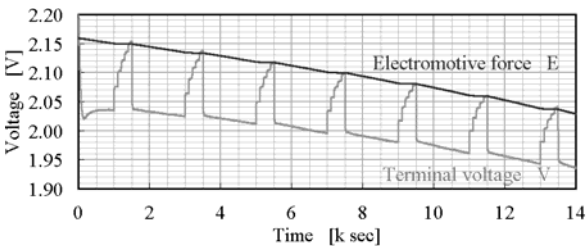

Fig.3.4: Estimated E during discharge examination

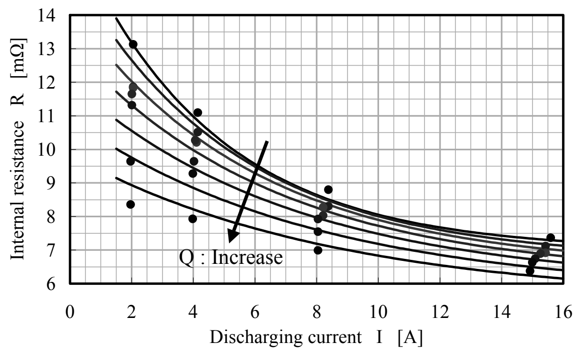

Fig.3.5: Dependence of internal resistance on I and Q

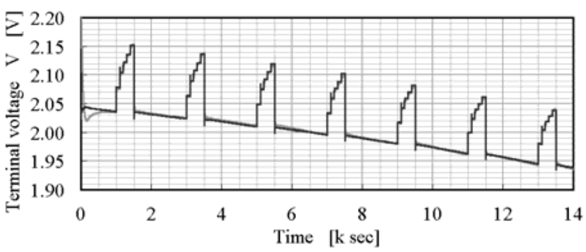

Fig.3.6: Simulated discharge characteristic of the battery

$$R = R_T \left(R_0 + R_1 \, e^{-\frac{I}{R_2}} \right) \qquad 3.6$$

$$R_T = R_{T_0} + R_{T_1} \, e^{-\frac{T}{R_{T_2}}} \qquad 3.7$$

$$R_0 = R_{0_0} - R_{0_1} \, Q \qquad 3.8$$

$$R_1 = R_{1_0} - R_{1_1} \, Q \qquad 3.9$$

$$R_2 = R_{2_0} + R_{2_1} \, Q \qquad 3.10$$

R_T is a function to rectify change by battery temperature T. R_{T0}, R_{T1} and R_{T2} are determined by other methods so that R_T may be set to 1 at 25 deg C of battery temperature. The result which determined other coefficients by the least-squares method is shown with curves in Fig.3.5.

Then terminal voltage during discharge examination can be simulated, and be shown in Fig.3.6. Even when current is small, it corresponds to the measurement result well and improvement in accuracy is accepted.

3.3 Electromotive force during charge

The relations between terminal voltage and charging current are obtained from charge characteristic shown in Fig.3.7 and are plotted on Fig.3.8, as a case of discharge. Since it is thought that a group of plots near full charge state is affected by electrolysis, it is ignored. Electromotive force is calculated from the 5 remaining groups by the same method as discharge, and is plotted on Fig.3.9.

It shows that electromotive force during charge is higher than one during discharge, and so difference of both is defined as E_d by the following formula.

$$E_d = E_{d_0} - E_{d_1} \exp\left\{ -E_{d_2} \left(1 - \frac{Q}{C_T} \right) \right\} \qquad 3.11$$

E_{d0}, E_{d1} and E_{d2} are determined by the least-squares method, thereby electromotive force during charge can be estimated in all discharge state.

3.4 Internal resistance during charge

Internal resistance is calculated by the formula 3.4, and is plotted on Fig.3.10. The dependence of it on the discharge state is examined by the same method as discharge. Consequently, it is thought appropriate that it is expressed with the following formulas.

$$R = R_T \left(Rc_0 + Rc_1 \, e^{\frac{I}{Rc_2}} \right) \qquad 3.12$$

$$Rc_0 = Rc_{0_0} + Rc_{0_1} \, e^{-Rc_{0_2} \, Q} \qquad 3.13$$

$$Rc_1 = Rc_{1_0} - Rc_{1_1} \, Q \qquad 3.14$$

$$Rc_2 = Rc_{2_0} + Rc_{2_1} \, Q \qquad 3.15$$

In a state near to full charge, terminal voltage rises suddenly. This is considered that the increase in internal resistance by the gas generation by electrolysis is the cause, and so gas generation function increasing exponentially is defined as G by the following formula.

$$G = G_0 \, e^{-G_1 \, Q} \qquad 3.16$$

And then the method of integrating discharging current and the method of calculating internal resistance are renewed.

$$Q(t) = Q(t_0) + (1 - G) \int_{t_0}^{t} I(t) \, dt \qquad 3.17$$

$$R = R_T \left(Rc_0 + Rc_1 \, e^{\frac{I}{Rc_2}} + R_g \, G \right) \qquad 3.18$$

A formula 3.17 is considering loss of the charge since charging current is used for electrolysis, and a formula 3.18 is calculating the increase in internal resistance by gas generation. They are fitted to a measured curve in Fig.3.11.

In Fig.3.12, the error is remaining at a state near full charge although electrolytic effect is being considered. It is thought that this cause is relating to quiescent time. The characteristic changes by the existence of quiescent time of

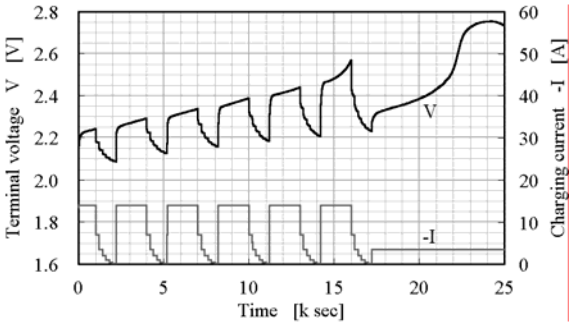

Fig.3.7: Measured charge characteristic of the battery

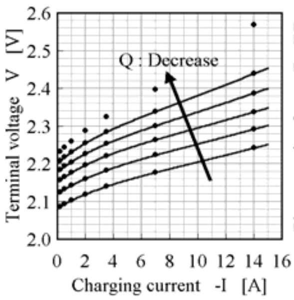

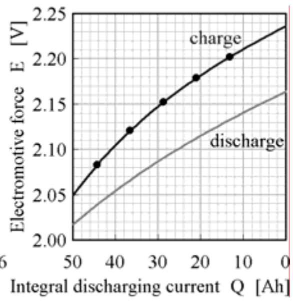

Fig.3.8: Calculating E Fig.3.9: Estimated E

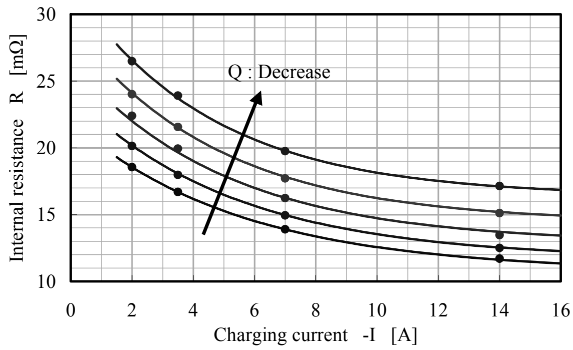

Fig.3.10: Dependence of internal resistance on I and Q

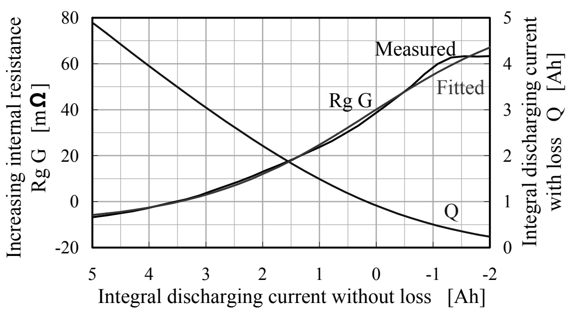

Fig.3.11: Estimation of electrolytic effect

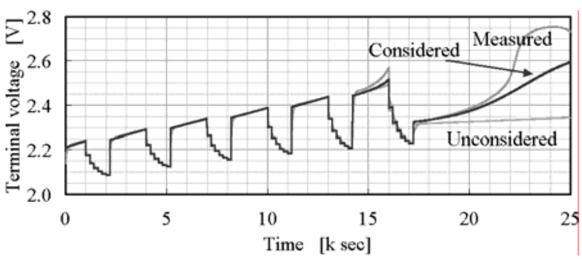

Fig.3.12: Simulated charge characteristic about electrolysis

even less than 1 hour. Therefore, if higher accuracy is searched for, it is thought that the battery model has to consider the effect of quiescent time.

4. SIMULATION

The simulation program of the whole system was developed, and it made the simulation for 10 days supposing the case where it installs in a ordinary residence. For the irradiance condition, the measured data of the fine weather day observed in Tsukuba (in Ibaraki JAPAN) was used. As the load data of a residence, the data which was measured in ordinary 5 residences for 82 days from January 9 to March 31, 2001 by Renewable Energy Promoting People's Forum was averaged every 10 minutes, and used. These data is shown in Fig.4. However, to check the simulation accuracy, the load data observed by the actual proof examination was given to the model input.

5. ACTUAL PROOF EXAMINATION

In this research, in order to check the simulation accuracy, the actual proof examination is being carried out. The power conditioner [LSS-4.5-S3C] and lead-acid batteries [SLC70] (128 V, 70 Ah) which we are using are standard equipments of Power Solar System made by Japan Storage Battery Co., Ltd. In order to secure the reproducibility of the experimental result, the photovoltaic array simulator made by Myway Labs Co., Ltd. and the residential load simulator made by author are being used. The same conditions were set up and measured.

6. RESULT

The simulation result is shown in Fig.5. Since the experimental result is almost the same as Fig.5, and is omitted. Electric energy which passes each part in the system per day is integrated according to direction, and both results are compared in Fig.6. The relative error is 1.0 % in a high item, 0.65 % on the whole. This error is 0.1 % as compared with the full scale of a measurement system. Therefore, it is thought that the simulation result with fully high accuracy was able to be obtained.

7. SUMMARY

About a lead-acid battery simulation, a possibility that accuracy could be vastly improved by modeling, being prepossessed without the conventional method was shown. Also the whole system can be simulated now with high precision, and can be used for designing new systems.

8. PROSPECTS

The lead-acid battery model continues to be considered. It is interesting if a transient response, the variation in the state of charge between batteries, the temperature rise by self-heating, and also the hysteresis in consideration of quiescent time can be estimated.

New systems, such as a system which utilizes solar radiation forecasting and demand forecasting for control, and can communicate with residents, are proposed, and are examined repeatedly from various viewpoints, such as economical efficiency, sociality, and global environmental problems, and the potential of the grid-connected photovoltaic system with battery is pursued.

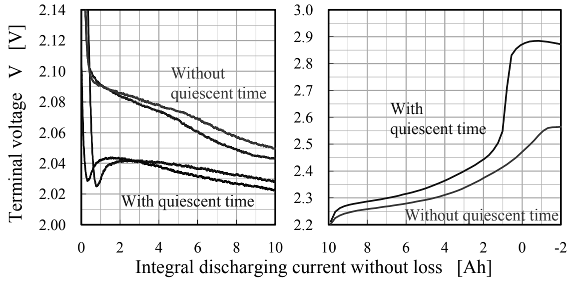

Fig.3.13: Dependence of characteristic on quiescent time

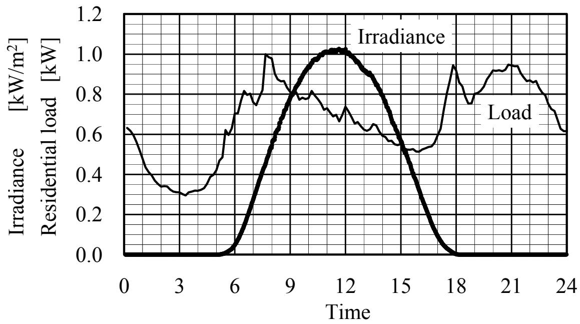

Fig.4: Irradiance data and residential load data

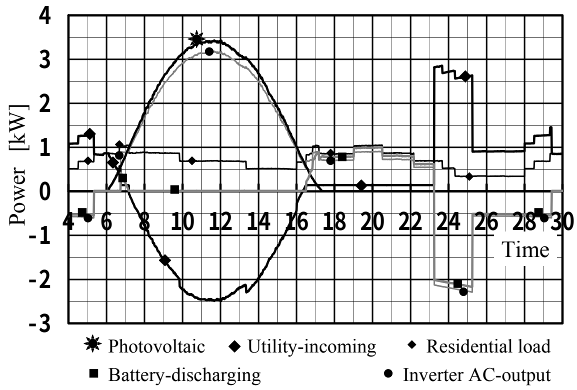

Fig.5: Simulation result

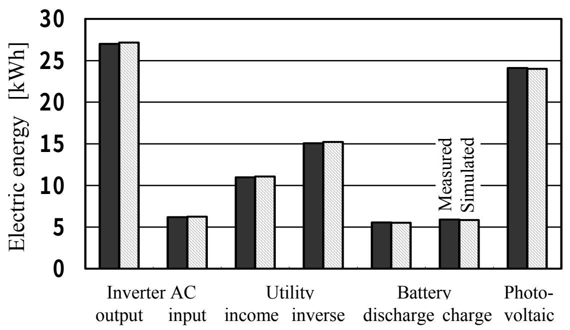

Fig.6: Passed electric energy per day

REFERENCES

[1] K. Kurokawa, S. Wakamatsu, Photovoltaic system design guidebook, Ohmsha, Ltd., ISBN 4-274-94065-9, 1994.
[2] Japanese industrial standards committee, Measuring method of output power for crystalline solar cells, JIS C 8913, 1998.